

Mapping of cost functions for the calibration of a lumped hydrological model and comparison of different minimization algorithms

Lorenzo Campo ¹, Andrea Cassioli ²

1. Dipartimento di Ingegneria Civile, University of Florence, E-mail: lcampo1@dicea.unifi.it, 2. Dipartimento di Sistemi e Informatica, University of Florence



1. The model

A simple lumped hydrological model was implemented in order to evaluate the performances of different cost functions and calibration algorithms. The model simulates rainfall infiltration, evapotranspiration, simple groundwater dynamics, small and large pore soil moisture dynamics, adsorption, percolation, hypodermic flow, base flow and hillslope flow. (see Figure 1). The model is able to simulate either a single rainfall-runoff event and the hydrological balance for a period of several years. The simple implemented numerical schemes (linear reservoirs, threshold infiltration, etc.) require in total four scalar parameters.

In this work this simple model was calibrated on three basins in central Italy (Ambra, Casentino, Sieve, see Figure 2), employing 4 different direct search algorithms (two local and two global) and 14 cost functions. The model was also used to map the different cost functions in order to highlight criticalities, if present, when these functions are used in a calibration procedure.

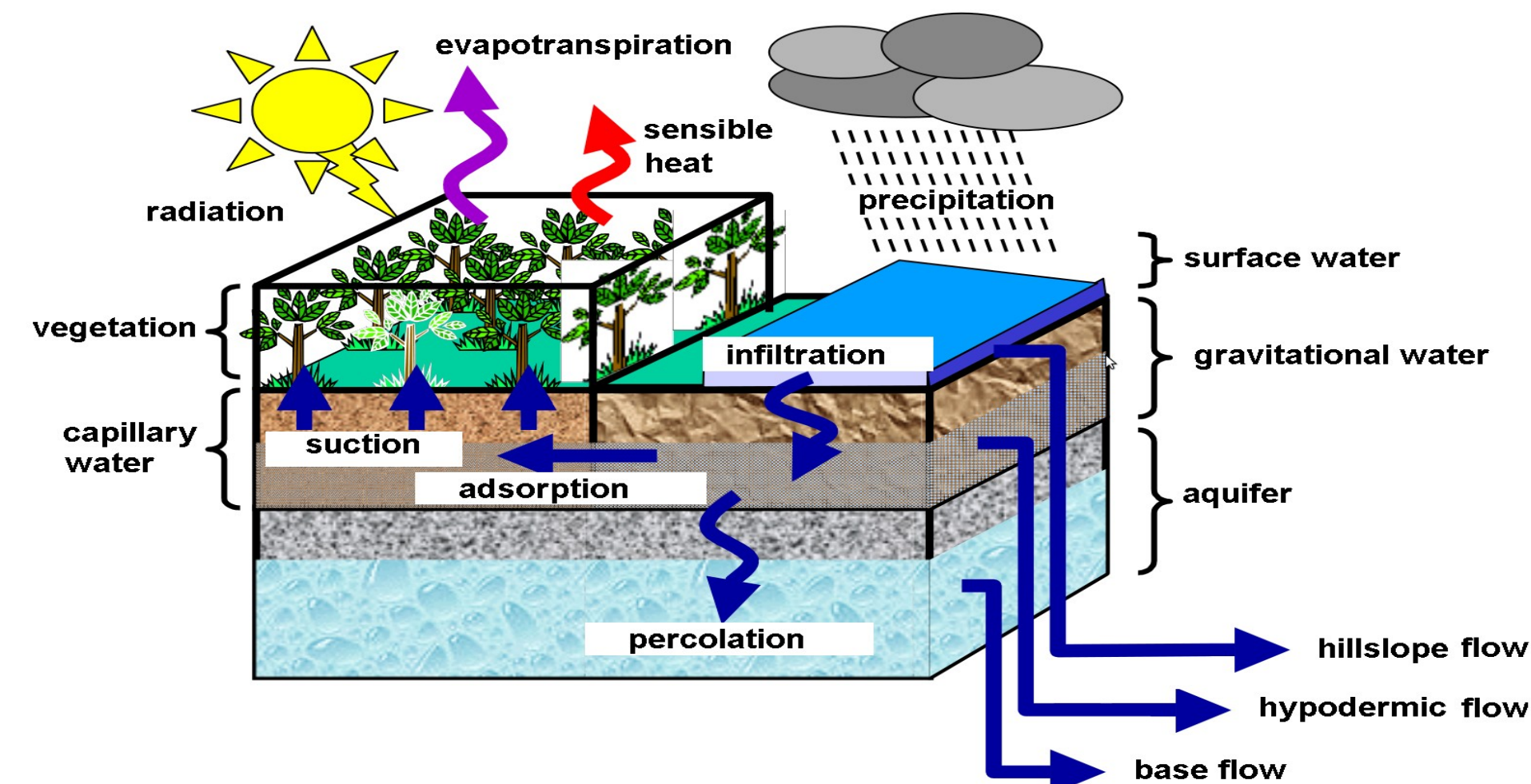


Figure 1. Schematic representation of the employed model.

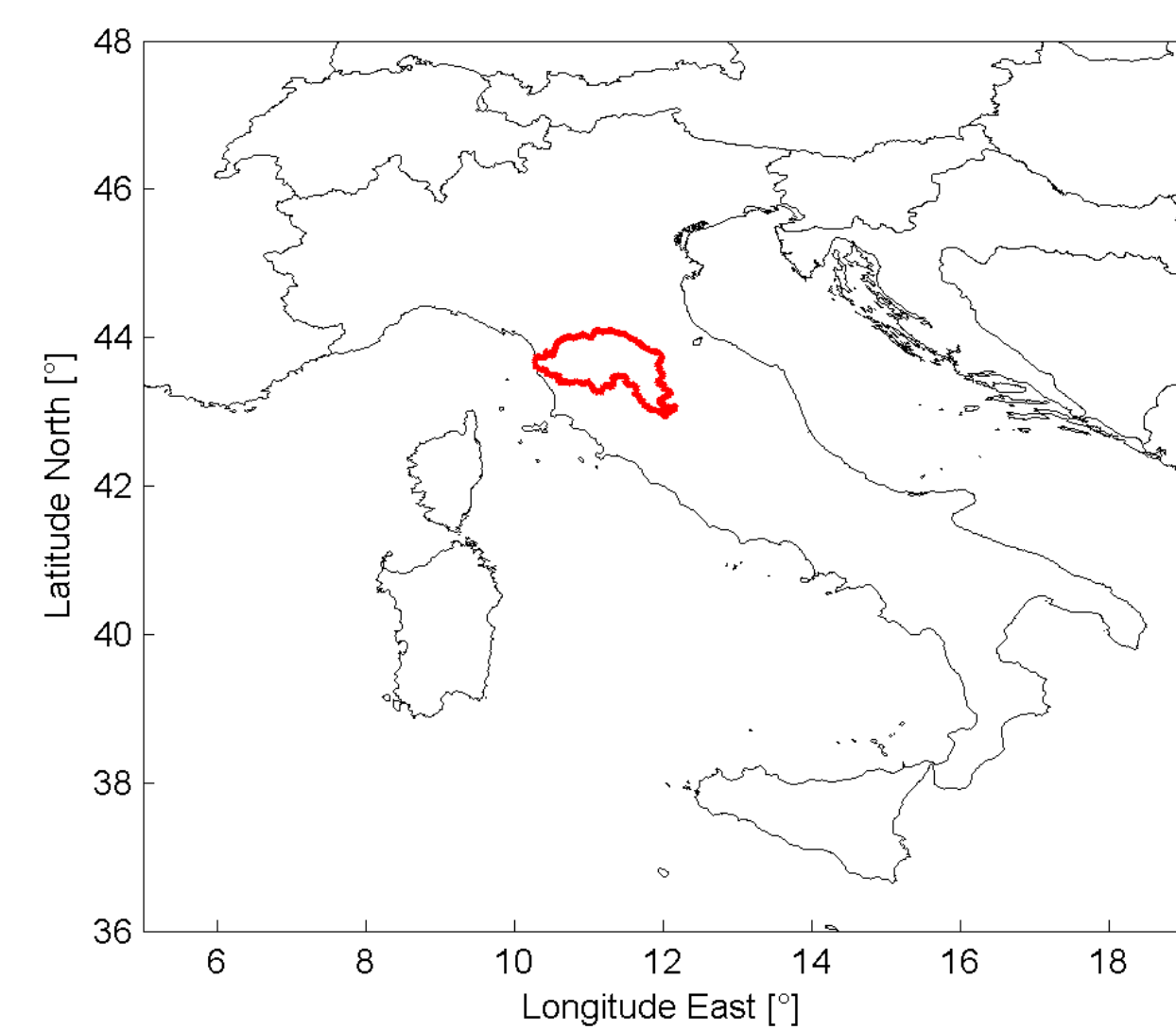


Figure 2a. Location of the Arno river basin in Central Italy.

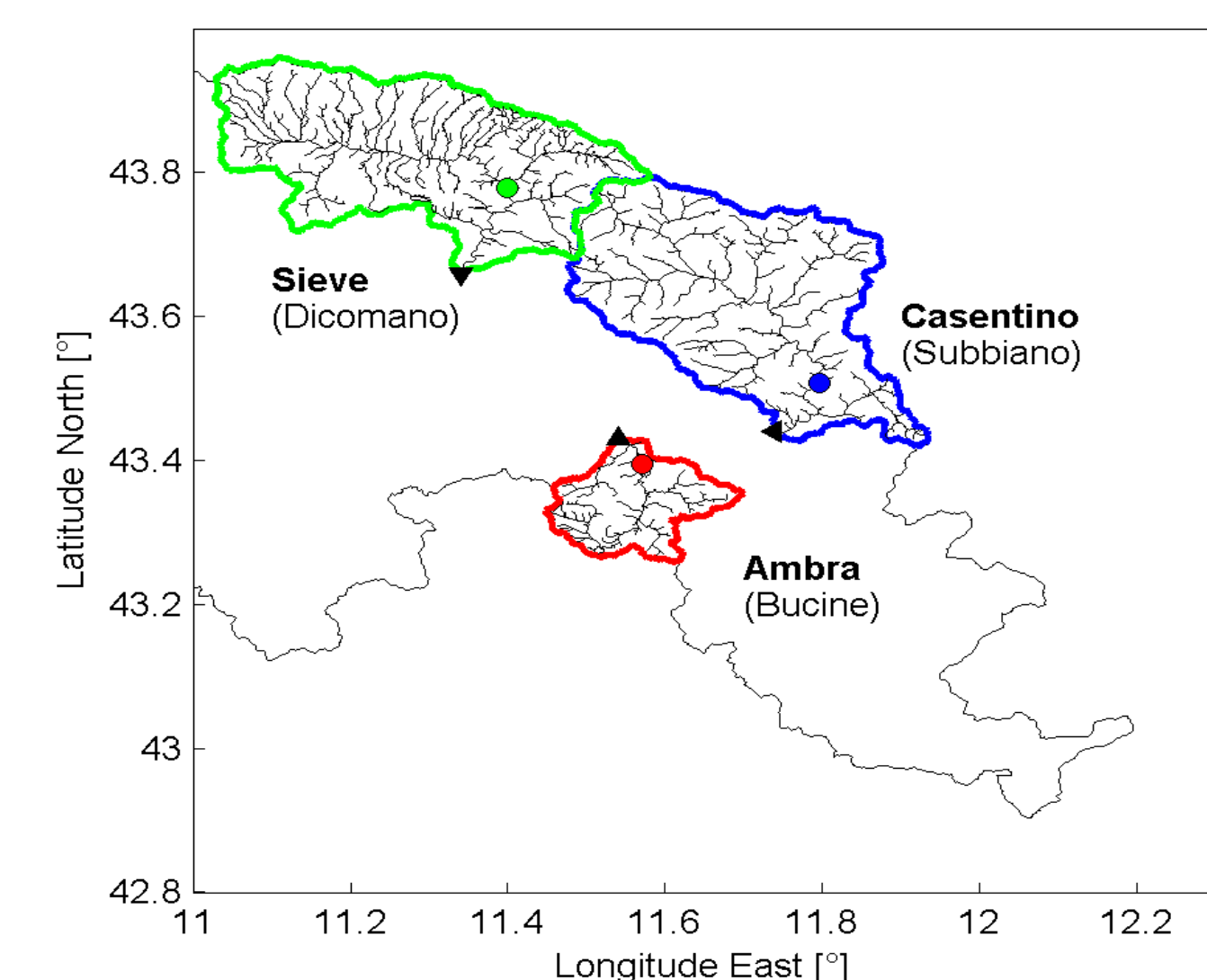


Figure 2b. Location of the three basins on which the model has been calibrated. Positions of the discharge flow gauges used for the observations are highlighted.

2. The calibration algorithms

The direct search family can be defined as that category of algorithms that make no use of derivatives of the cost function (that is, in general, a black box) and comprehend a large number of possible approaches.

The first algorithm is the classical Nelder-Mead, in which a simplex is used to explore the parameter space to search for the maximum descent direction. The second one is a GSS (Generating Set Search) algorithm, in which a rotating and expanding/contracting n-dimensional cross is used to search for the minimum. In this work the rotation of the cross was avoided. The third one is the EGO algorithm (Efficient Global Optimization), that performs a global optimization searching for the maximum of the Expected Improvement (EI) function:

$$E[I(x)] = (f_{\min} - \hat{y})\Phi\left(\frac{f_{\min} - \hat{y}}{s}\right) + s\phi\left(\frac{f_{\min} - \hat{y}}{s}\right)$$

where f_{\min} represents the current best value of the cost function, \hat{y} and s are mean and standard deviation of the predictor of the model (the interpolation model) in the position x and ϕ and Φ are respectively the PDF and the CDF of the normal distribution $N(\theta, 1)$. EI function represents the improvement in the cost function that is expected given a set of explored points in parameters space and the error of the interpolation surface (here obtained with a kriging technique) that represents the response surface of the model. The last algorithm is the Gutmann algorithm in which a response surface is fitted using radial basis functions. In Figures 3 the algorithms are used to find the minimum of a simple 2-variables function.

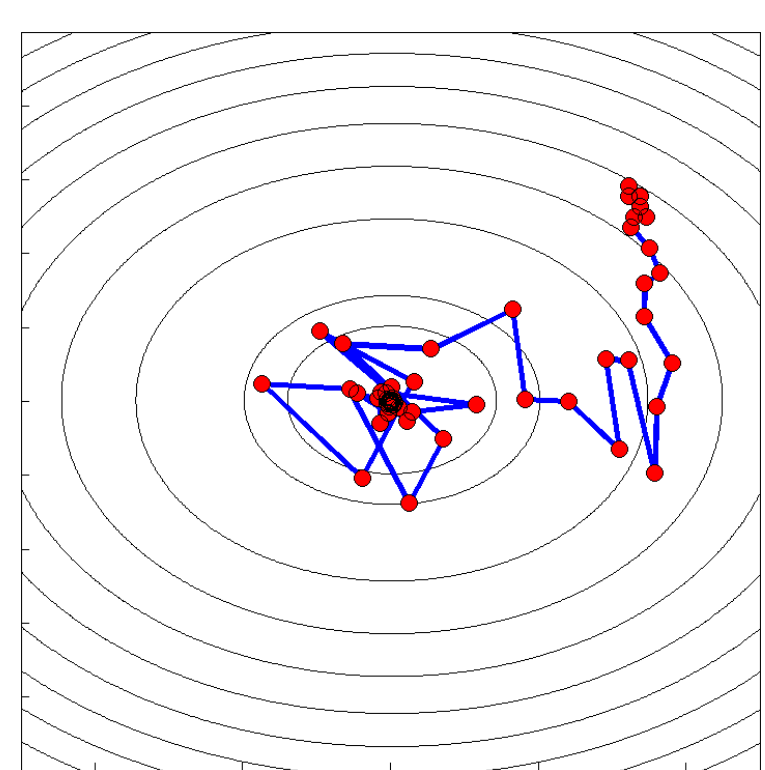


Figure 3a. Trajectory of the Nelder-Mead algorithm.

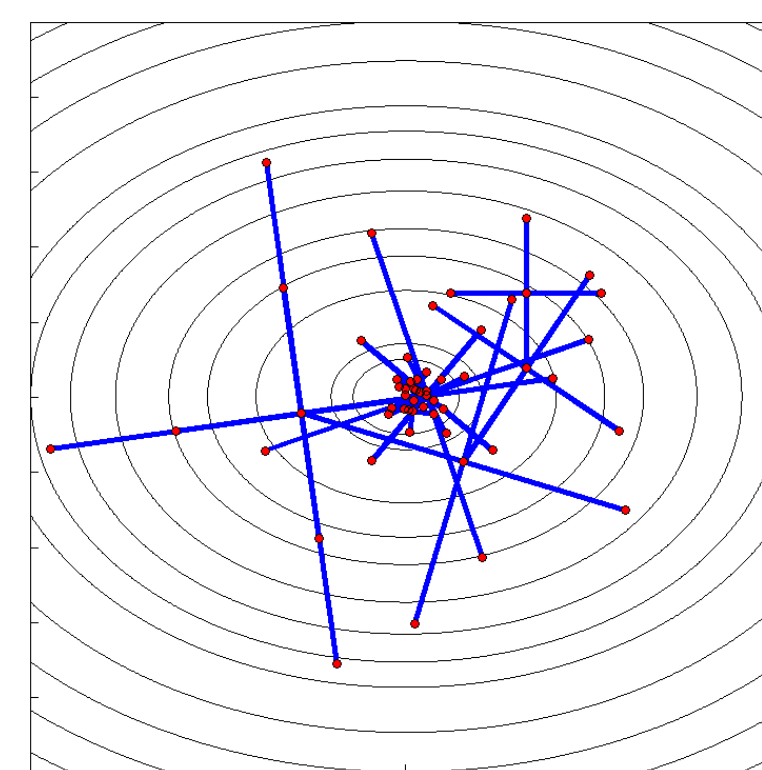


Figure 3b. Trajectory of the GSS rotating cross algorithm.

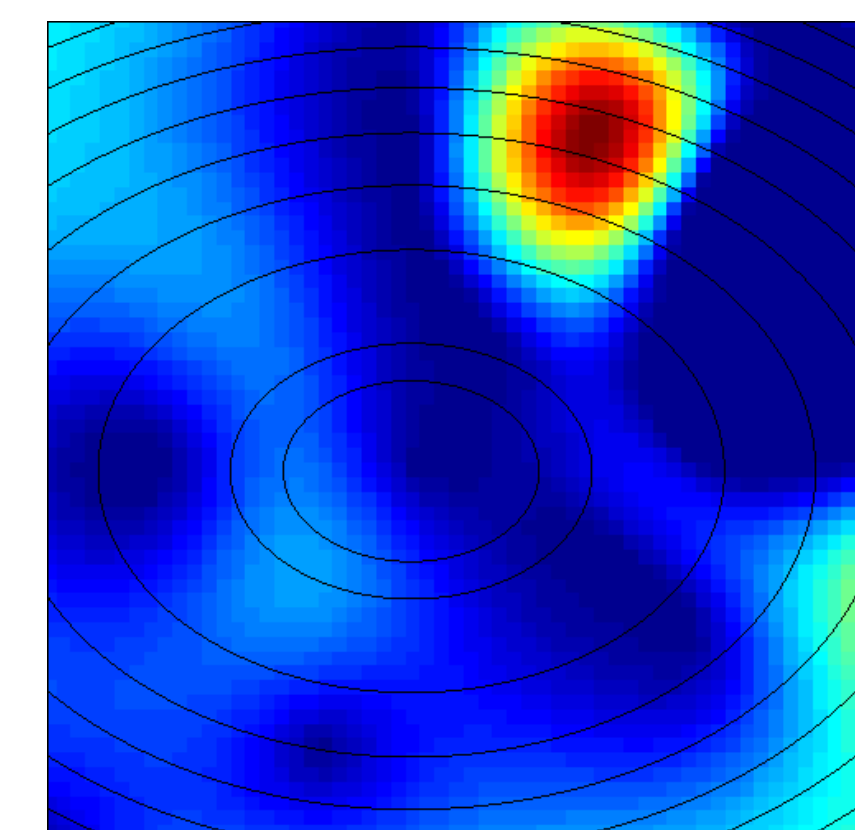


Figure 3c. Expected Improvement surface from the EGO algorithm.

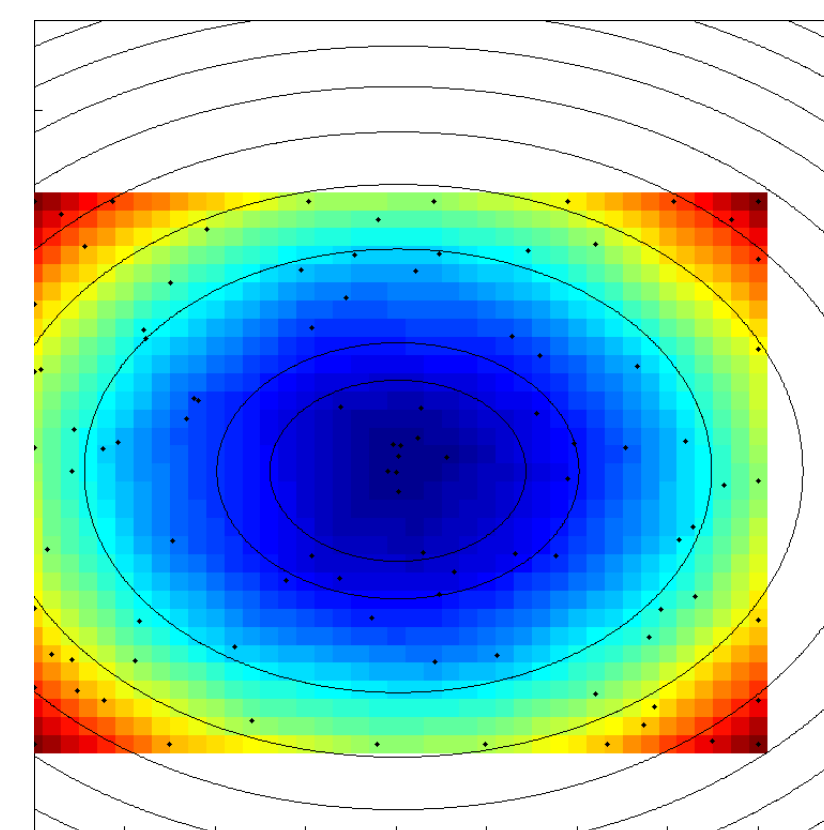


Figure 3d. Response surface obtained with the Gutmann algorithm.

3. The cost functions

In all three considered basins the following four parameters were calibrated: α = hillslope flow coefficient [1/s], β = hypodermic flow coefficient [1/s], γ = percolation coefficient [1/s], κ = adsorption coefficient [1/s]. The calibration was performed by minimizing the following 14 cost functions, in which Q_m and Q_s are observed and simulated discharge flows at the gauges represented in Figure 2b, $P_\alpha(p)$ are the p-percentiles and w_β are Gaussian coefficients. The comparison was made on the whole 2005.

- 1) $J = \frac{1}{n} \sum_{t=1}^n |Q_s(t) - Q_m(t)|$
- 2) $J = \frac{1}{n} \sum_{t=1}^n (Q_s(t) - Q_m(t))^2$
- 3) $J = \frac{1}{n} \sum_{t=1}^n |Q_s(t) - Q_m(t)|^p$
- 4) $J = \frac{1}{n} \sum_{t=1}^n \left| \log \left(\frac{Q_s(t) + Q_{\min}}{Q_m(t) + Q_{\min}} \right) \right|$
- 5) $J = \frac{1}{n} \sum_{t=1}^n (Q_{s,\text{gms}}(t) - Q_{m,\text{gms}}(t))^2 \quad Q_{m,\text{gms}}(t) = \frac{1}{5} \sum_{i=2}^5 Q_m(t)$
- 6) $J = \frac{1}{n} \sum_{t=1}^n (Q_{s,\text{gms}}(t) - Q_{m,\text{gms}}(t))^2 \quad Q_{m,\text{gms}}(t) = \sum_{i=2}^5 w_\beta |t - i| Q_m(t)$
- 7) $J = \frac{1}{n} \sum_{p=1}^{100} |P_\alpha(p) - P_\alpha^o(p)|$
- 8) $J = \frac{1}{n} \sum_{p=1}^{100} (P_\alpha(p) - P_\alpha^o(p))^2$
- 9) $J = \frac{86400}{n} \sum_{t=1}^n \left(\sum_{i=1}^n Q_s(t) - \sum_{i=1}^n Q_m(t) \right)^2$
- 10) $J = 1 - \frac{\sum_{t=1}^n (Q_m(t) - Q_s(t))^2}{\sum_{t=1}^n (Q_m(t) - \bar{Q}_m)^2}$
- 11) $J = 1 - \frac{\sum_{t=1}^n \left(\frac{Q_m(t) - Q_s(t)}{Q_m(t)} \right)^2}{\sum_{t=1}^n \left(\frac{Q_m(t) - \bar{Q}_m}{Q_m(t)} \right)^2}$
- 12) $J = 1 - \frac{\sum_{t=1}^n (Q_s(t) - \bar{Q}_s) (Q_m(t) - \bar{Q}_m)}{\sqrt{\sum_{t=1}^n (Q_s(t) - \bar{Q}_s)^2 \sum_{t=1}^n (Q_m(t) - \bar{Q}_m)^2}}$
- 13) $J = \frac{\sum_{t=1}^n (Q_s(t) - Q_m(t))^2}{\sum_{t=1}^n (|Q_s(t) - \bar{Q}_s| + |Q_m(t) - \bar{Q}_m|)^2}$
- 14) $J = \frac{\sum_{t=1}^n (Q_s(t) - Q_m(t))^2}{\sum_{t=1}^n \left(\frac{|Q_s(t) - \bar{Q}_s| + |Q_m(t) - \bar{Q}_m|}{Q_m(t)} \right)^2}$

Cost functions mapped for Ambra basin

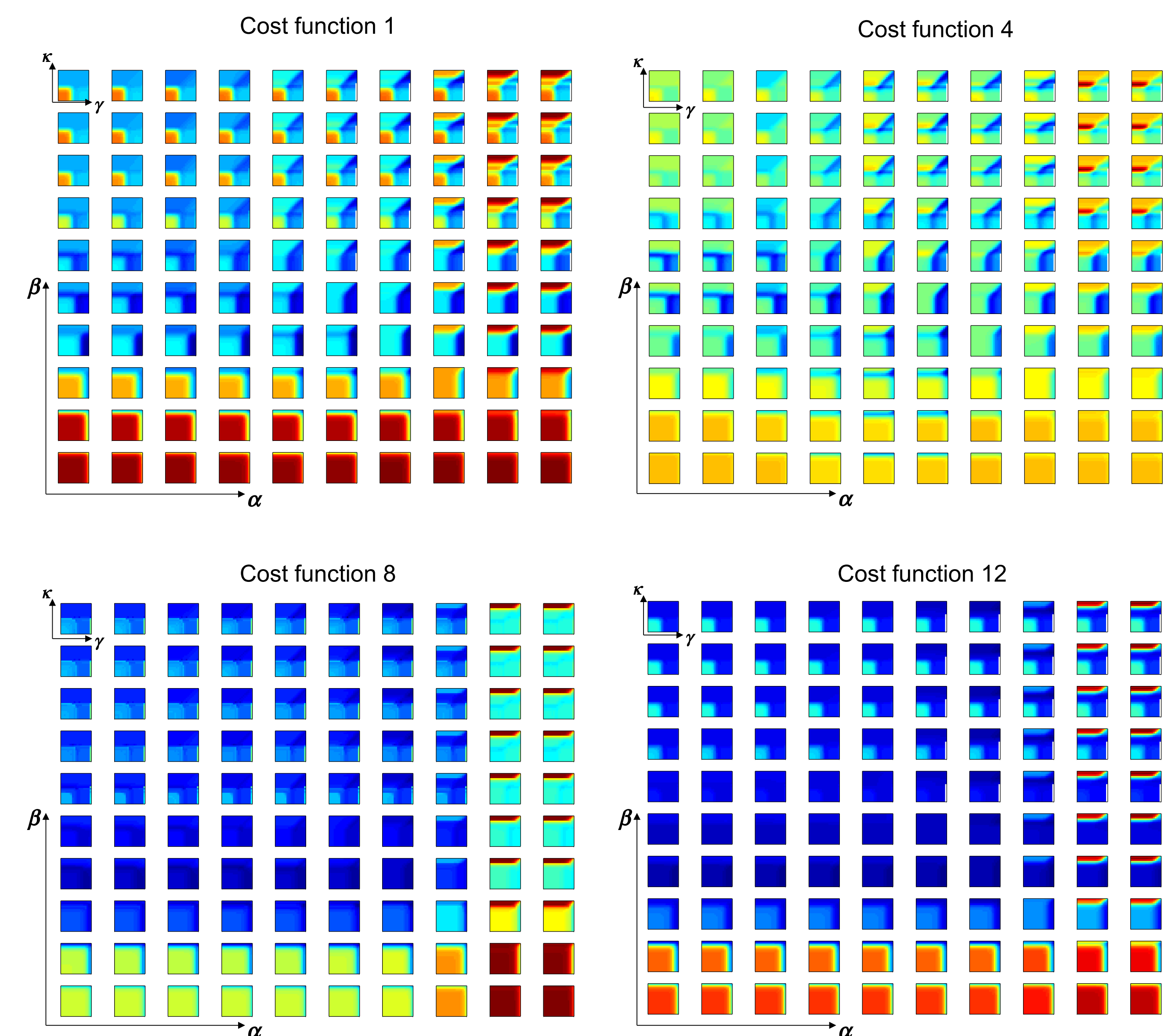


Figure 4. 4-Dimensional mapping of the cost functions 1, 4, 8 and 12. For each case several 2-D sections at constant α and β are shown. In each section γ and κ are represented on x-axis and y-axis respectively.

4. Results

The evaluation of the calibration procedures was performed considering both the number of required evaluations (not considering the required initial filling for what concerns EGO) of the cost functions and the distance from the actual optimum. The algorithms NM and GSS were used with a multi-start approach, so the average number of evaluations is represented. The results are summarized in Figures 5a,b,c. The figures show that different algorithms reached different optima, in particular cost functions 12 and 13 in general failed to obtain an acceptable estimation of the optimal parameters. GSS resulted the most efficient algorithm.

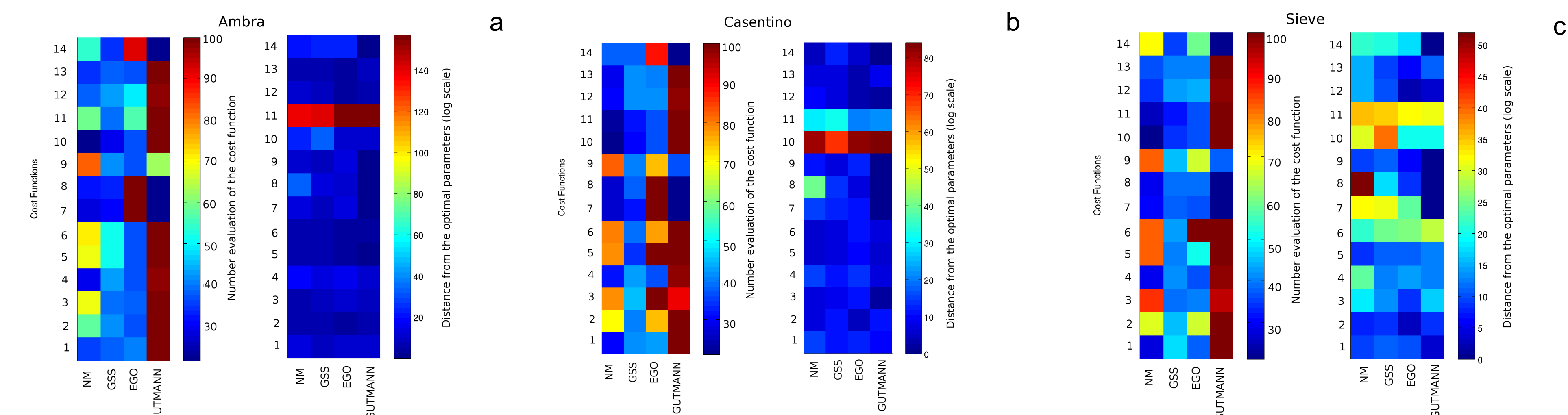


Figure 5. Number of evaluations (left) and distance from the actual optimum (log distance in parameters space, on the right) for Ambra (a), Casentino (b) and Sieve basin (c).